



Time domain analysis of vibrations induced by dynamic loads in tunnels

Carlos Albino¹, Luís Godinho¹, Daniel Dias-da-Costa²

¹ University of Coimbra, ISISE, Department of Civil Engineering, Coimbra, Portugal.
capa@uc.pt, lgodinho@dec.uc.pt

² School of Civil Engineering, The University of Sydney, Sydney, Australia.
daniel.diasdacosta@sydney.edu.au

Abstract

Vibration induced by heavy vehicles is a significant problem in large cities causing a major impact on human activities, comfort and health. The quantification of the vibrations in a building is essential for the definition of mitigation strategies. As a significant example, consider the underground railway systems that induce vibrations in tunnels that propagate to the surrounding soil and can disturb, in the form of vibration, the inhabitants of the adjacent buildings. In this paper, the authors intend to simulate the effect of a dynamic load on the tunnel base and the consequent vibration propagation in the ground and the building structure. Parametric studies are presented for different propagation scenarios. The effects of mitigation measures such as trenches, buried walls and phononic crystals horizontally arranged are evaluated. The simulations are performed using a 2D finite element model, formulated in the time domain and using a time-marching algorithm that allows an efficient calculation procedure.

Keywords: Numerical modelling, Phononic crystals, Time marching, Underground-tunnels railway, Vibration mitigation.

1 Introduction

Mitigation of mechanical waves originating in heavy transport traffic is currently an extremely important topic in Civil Engineering. Both the surface and the underground-tunnels railway systems are the main sources of vibration that propagate to the surrounding soil and can directly interfere with adjacent buildings and human comfort and well-being. Recently, researchers have developed new and innovative methods based on a physical concept already widely known in the acoustics world, more specifically in the acoustic barriers' development. These barriers are constituted by elements arranged periodically that are commonly known as "sonic" or "phononic" crystals [1] and have a significant effect on vibration levels reduction, mainly in the downstream zone. As a group of inclusions with the same characteristics, these barriers are only efficient in a certain frequency range. By changing some crystalline parameters, such as the distance between inclusions, their geometry, or their distribution within the phononic crystal, it is possible to move, reduce or enlarge the frequency range for which the barrier is most efficient. An optimal and tuned system depends widely on the properties of the host medium, the properties of the inclusions and the frequency band to be mitigated. Each configuration has its efficiency zone very much enhanced in the band gap frequency range [2].

The present paper follows previous works by the authors in which numerical simulations are used to better understand the propagation of vibrations, originating from the surface railways, and the mitigation that those periodic buried structures provide on vibration levels [1,3–6]. Here, to help simulate the effect of the

inclusion of those periodic structures, an innovative time marching algorithm supported by the 2D finite element method was used [7].

2 Wave propagation

In a solid material excited by mechanical impulses, three important types of waves are generated. The compression waves (P) are those with the highest propagation velocity, defined by equation (1) (E , ν and ρ being the Young's modulus, Poisson's ratio and density). Those are longitudinal waves causing displacements in the medium, parallel to the direction of the wave. The shear waves (S) are transverse waves causing displacements in the medium, and they are perpendicular to the direction of the propagation. These waves are slower than P waves and their speed is defined by equation (2). The surface waves are the slowest. For its low frequency, long duration, and large amplitude these can usually be the most destructive. There are several types of surface wave (such as Rayleigh and Love). For the Rayleigh (R) waves, which propagate along the surface, their velocity is approximately that defined in equation (3). These waves cause elliptical orbit displacements in the medium particles and their amplitude decreases rapidly with depth.

$$v_P = \sqrt{\frac{E(1-\nu)}{\rho(1+\nu)(1-2\nu)}} \quad (1)$$

$$v_S = \sqrt{\frac{E}{2\rho(1+\nu)}} \quad (2)$$

$$v_R = \frac{0.87+1.12\nu}{1+\nu} \sqrt{\frac{E}{2\rho(1+\nu)}} \quad (3)$$

3 Numerical Model

In this work it is intended to study the full wavefield generated when the train passes in an embankment railway and in an underground-tunnel railway. A loading line is used to simulate the excitation source. The 2D finite element method (FEM) is here used in the time domain, to simulate several scenarios. This method, applied to a dynamic, multidimensional, and damped system, can be mathematically defined by the equation (4).

$$\mathbf{F} = \mathbf{F}_I + \mathbf{F}_D + \mathbf{F}_S \quad (4)$$

where $\mathbf{F} = \mathbf{F}(t)$ is the applied load, $\mathbf{F}_I = \mathbf{M}\dot{\mathbf{U}}(t)$ is the force of inertia, $\mathbf{F}_D = \mathbf{C}\dot{\mathbf{U}}(t)$ is the damping force (considering a viscous damping) and $\mathbf{F}_S = \mathbf{K}\mathbf{U}(t)$ is the elastic force. \mathbf{M} , \mathbf{C} and \mathbf{K} , are respectively the mass, damping and stiffness matrices. $\ddot{\mathbf{U}}(t)$, $\dot{\mathbf{U}} = \dot{\mathbf{U}}(t)$ and $\mathbf{U} = \mathbf{U}(t)$, are respectively the acceleration, velocity, and displacement vectors dependent on time, t . Once \mathbf{M} , \mathbf{C} and \mathbf{K} matrices are obtained, the time integration is performed with an innovative algorithm, developed by Soares Jr., presented in [7], where the basic aspects and the main parameters of the new time-marching formulation are described. This paper presents only the time-marching equations used in this new formulation, which are

$$\mathbf{E}\dot{\mathbf{U}}^{n+1} = \mathfrak{S}_F^{n+\frac{1}{2}} + \mathbf{M}\dot{\mathbf{U}}^n - \frac{1}{2}\Delta t\mathbf{C}\dot{\mathbf{U}}^n - \mathbf{K}\left(\Delta t\mathbf{U}^n + \frac{1}{2}\Delta t^2\ddot{\mathbf{U}}^n\right) \quad (5)$$

– the velocity equation – and

$$\mathbf{E}\mathbf{U}^{n+1} = \mathbf{E}\left(\mathbf{U}^n + \frac{1}{2}\Delta t\dot{\mathbf{U}}^n + \frac{1}{2}\Delta t\dot{\mathbf{U}}^{n+1}\right) - \frac{1}{2}\Delta t^2\mathbf{C}\dot{\mathbf{U}}^{n+1} - \mathbf{K}\left[(\beta b_1 b_2)\Delta t^3\ddot{\mathbf{U}}^n + \left(\frac{1}{16} + \beta b_1\right)\Delta t^3\ddot{\mathbf{U}}^{n+1}\right] \quad (6)$$

– the displacement equation – where $\mathbf{E} = \mathbf{M} + \frac{1}{2}\Delta t\mathbf{C}$ is the effective matrix; n and Δt are the time-step number and time-step length, respectively; $\beta = 1$, $b_1 = 8.567 \times 10^{-3}$ and $b_2 = 8.590 \times 10^{-1}$ are the time integration

parameters of the new method; $\mathfrak{F}_F^{n+1/2} = \beta_1 \Delta t F^n + \beta_2 \Delta t F^{n+1}$, with $\beta_1 = \beta_2 = 1/2$, using trapezoidal quadrature rule or $\beta_1 = 1$ and $\beta_2 = 0$, extending the explicit feature of the technique to the load term (see [7] for more details).

The main features of this model, among others, are: the method is based only on single-step displacement-velocity relations; it requires no system of equations to be dealt with; it is second-order accurate. In other words, this model is very effective, being able to provide accurate analyses considering relatively large time steps (thus, also being very efficient). Moreover, since it has high stability limits, it minimizes the main drawback of explicit procedures, allowing time-steps that are usual in accurate implicit analyses, rendering good results at reduced computational costs [7].

4 Numerical results

As mentioned in the Introduction, this article is following previous work of the authors. Here, an important aspect is introduced, namely the effect of the vibration source being a few metres below the ground surface in the wave propagation patterns and, in the protection, provided by mitigation devices. To evaluate the effect of such parameters on the vibrations registered at different receivers, the insertion loss was computed for several scenarios and then the results were compared with those obtained for a reference medium.

The evaluated mitigation devices correspond to trenches, buried walls, phononic crystals and combinations of buried walls with phononic crystals. Figure 1 and Figure 2 show the schematic representation of the models used for the analysis where the propagation sources can be seen, centred horizontally on top of an embankment and inside a tunnel, respectively. In these figures, the relative location of the embankment and the tunnel, the mitigation zone, and the nearest building, can be seen. Also, all measurements and relative distances of the system are defined in these figures. The material properties are defined in Table 1 and the mitigation devices that will take place, each in turn, in the mitigation zone are represented in Figure 3 and described in Table 2. Mitigation devices are 0.6 m wide. Trenches and walls have different depths and inclusions have a square section and are placed at different depths (see Figure 3).

Since the propagation domain is semi-infinite, an absorbent layer was considered based on progressively increasing the material damping towards the outer limits of the model. This layer is responsible for absorbing all the energy that enters it, avoiding unwanted reflections in the system under study. An absorption layer 1.5 times the wavelength of the host medium is sufficient to absorb all the unwanted reflections. In this specific case, an absorbent layer 8 m wide is required.

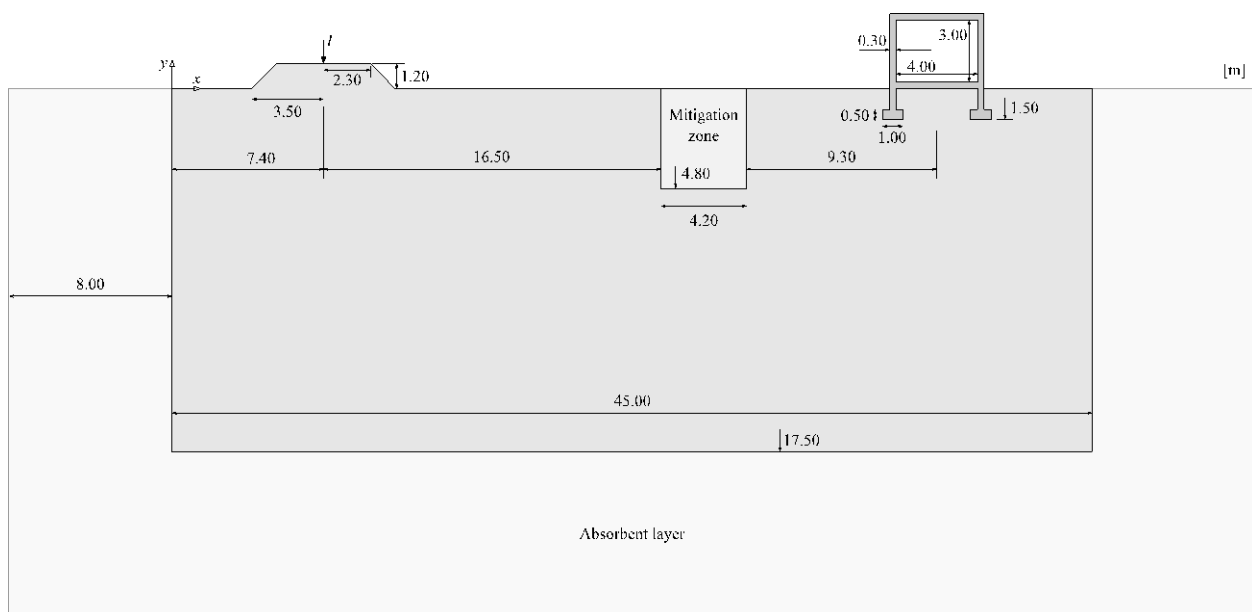


Figure 1 – Schematic representation of the embankment model used for the analysis of wave propagation.

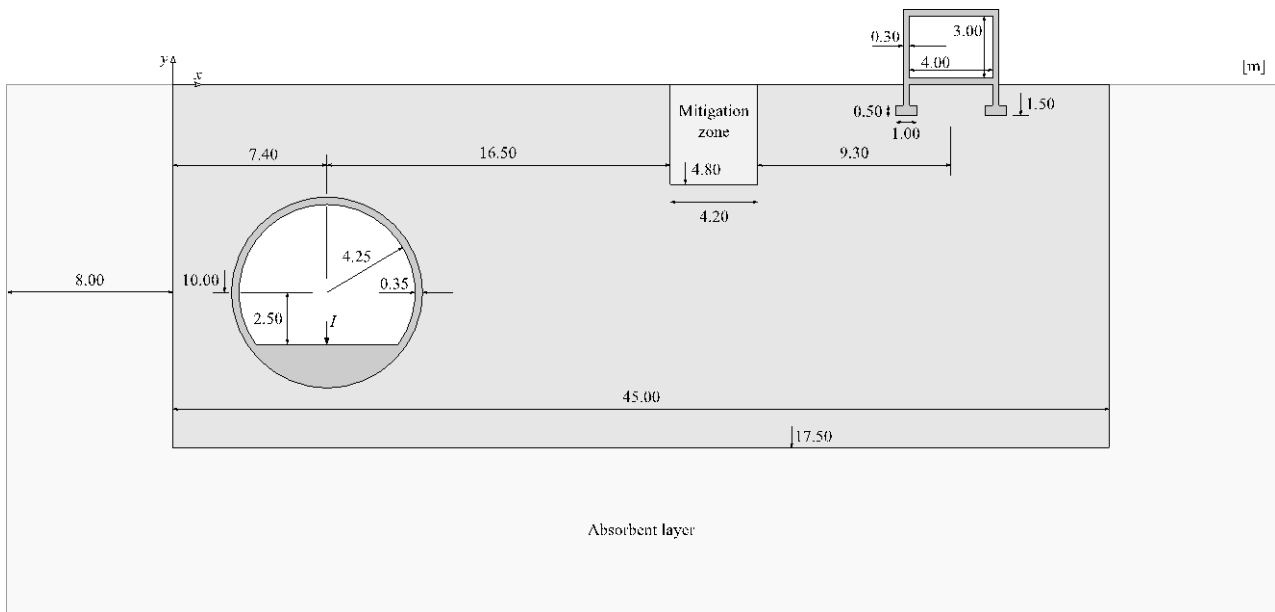


Figure 2 – Schematic representation of the tunnel model used for wave propagation analysis.

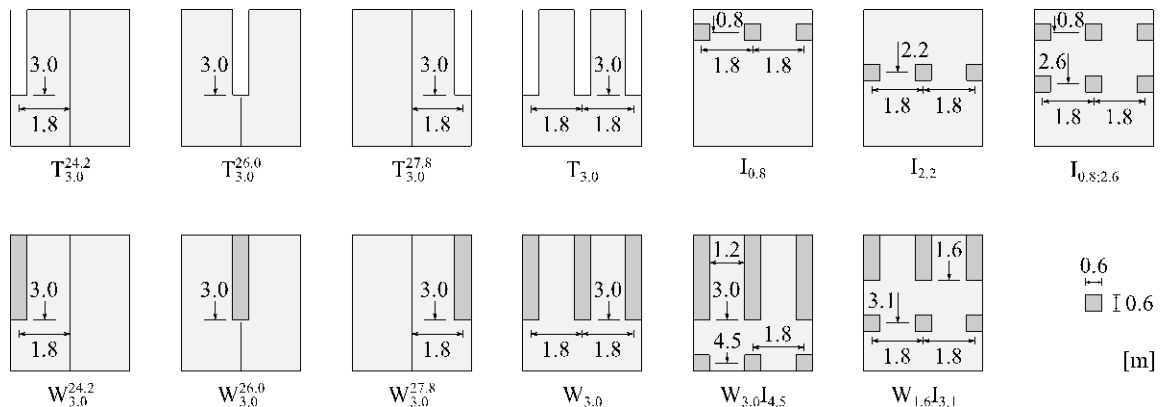


Figure 3 – Schematic representation of the mitigation devices.

In both models, the system is excited by a Ricker pulse generated by a source located 7.40 m right of the system origin (see Figure 1 and Figure 2) and the evaluation is carried out by analysing the vibrations recorded in three groups of receivers placed in strategic positions (see Figure 4): (1) on the ground surface just before the building, (2) on the base of the building and (3) on the top of the building.

Table 1 – Material properties.

Material	Density [kg/m ³]	Poisson's ratio	Young's modulus [Pa]	Wave velocities [m/s]		
				P	S	R
Host medium	1700	0.33	115.76×10 ⁶	318	160	149
Tunnel concrete	2500	0.20	35×10 ⁹	3944	2415	2202
Building concrete	2500	0.20	31×10 ⁹	3712	2273	2072
Buried mitigation devices (poor)	2100	0.25	2.7×10 ⁹	1242	717	660
Buried mitigation devices (stiff)	2400	0.20	27×10 ⁹	3536	2165	1974

Table 2 – Description of mitigation devices.

Reference	Description
$T_{3.0}^{24.2}$	Trench at position $x=24.2$ m with a depth of 3.0 m.
$T_{3.0}^{26.0}$	Trench at position $x=26.0$ m with a depth of 3.0 m.
$T_{3.0}^{27.8}$	Trench at position $x=27.8$ m with a depth of 3.0 m.
$T_{3.0}$	Group of 3 trenches centred at $x=26.0$ m with a depth of 3.0 m.
$W_{3.0}^{24.2}$	Wall at position $x=24.2$ m with a depth of 3.0 m.
$W_{3.0}^{26.0}$	Wall at position $x=26.0$ m with a depth of 3.0 m.
$W_{3.0}^{27.8}$	Wall at position $x=27.8$ m with a depth of 3.0 m.
$W_{3.0}$	Group of 3 walls centred at $x=26.0$ m with a depth of 3.0 m.
$W_{3.0}I_{4.5}$	Group of 3 walls and 3 inclusions centred at $x=26.0$ m with a depth of 3.0 m and 4.5 m, respectively.
$W_{1.6}I_{3.1}$	Group of 3 walls and 3 inclusions centred at $x=26.0$ m with a depth of 1.6 m and 3.1 m, respectively.
$I_{0.8}$	Group of 3 inclusions, horizontally distributed, centred at $x=26.0$ m with a depth of 0.8 m.
$I_{2.2}$	Group of 3 inclusions, horizontally distributed, centred at $x=26.0$ m with a depth of 2.2 m.
$I_{0.8;2.6}$	2 groups of 3 inclusions, horizontally distributed, centred at $x=26.0$ m with a depth of 0.8 m and 2.6, respectively.

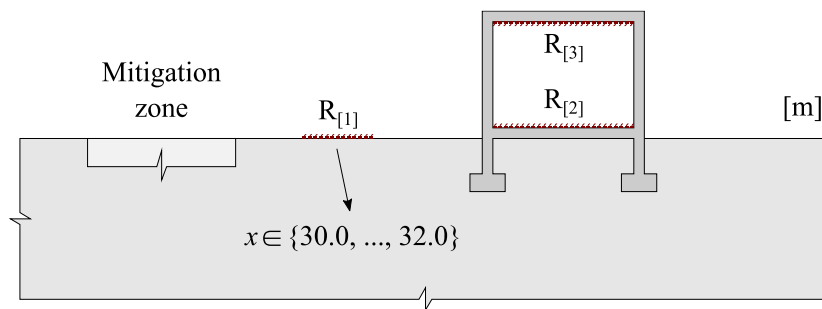


Figure 4 – Location of receivers.

Numerical simulations were performed using a 2D FEM in the time domain, formulated with an average of 87 566 triangular elements, whose longest edge is 0.31 m, fitting 8 elements per wavelength. This mesh was obtained from the Gmsh program (version 4.8.4). The time marching algorithm described above was developed by Soares Jr. [7] and is adopted to render the numerical process more efficient. A damping factor equal to 1% and a propagating Ricker pulse with a central frequency of 60 Hz were considered.

Before making a deeper analysis, the average vertical vibration levels detected in the different sets of receivers, defined in Figure 4, for each model (embankment railway and the underground tunnel railway) are shown in Figure 5. This figure also shows the reference vertical vibration level considering the load applied to the soil surface (solid black line). Figure 4 (a) shows the average levels for the receivers $R_{[1]}$, Figure 4 (b) shows the average levels for the receivers $R_{[2]}$, and Figure 4 (c) shows the average levels for the receivers $R_{[3]}$. In general, the registered levels are lower than the reference levels and the levels originating in the tunnel are always lower. However, in the embankment railway model, the levels recorded in the receivers before the building are found to be higher than the reference levels.

An analysis of the results by type of mitigation device is presented here, comparing the two models: the embankment railway and the underground tunnel railway. To evaluate the effect of the presence of mitigation devices in the vibrations registered in the previously mentioned receivers, the reduction is computed in terms of insertion loss, IL , which is defined as the difference between the vibration levels obtained in the presence of mitigation devices ($L1$) and the displacement vibration levels obtained without those devices ($L0$). This is given in dB by the following equation 7:

$$IL = L_0 - L_1 = 20 \log|u_0| - 20 \log|u_1| \quad (7)$$

where u_i are the vertical displacements amplitude. According to equation 7, positive values correspond to a reduction of the displacement vibration levels in the presence of mitigation devices and negative values of the insertion loss stand for losing protective solutions efficiency.

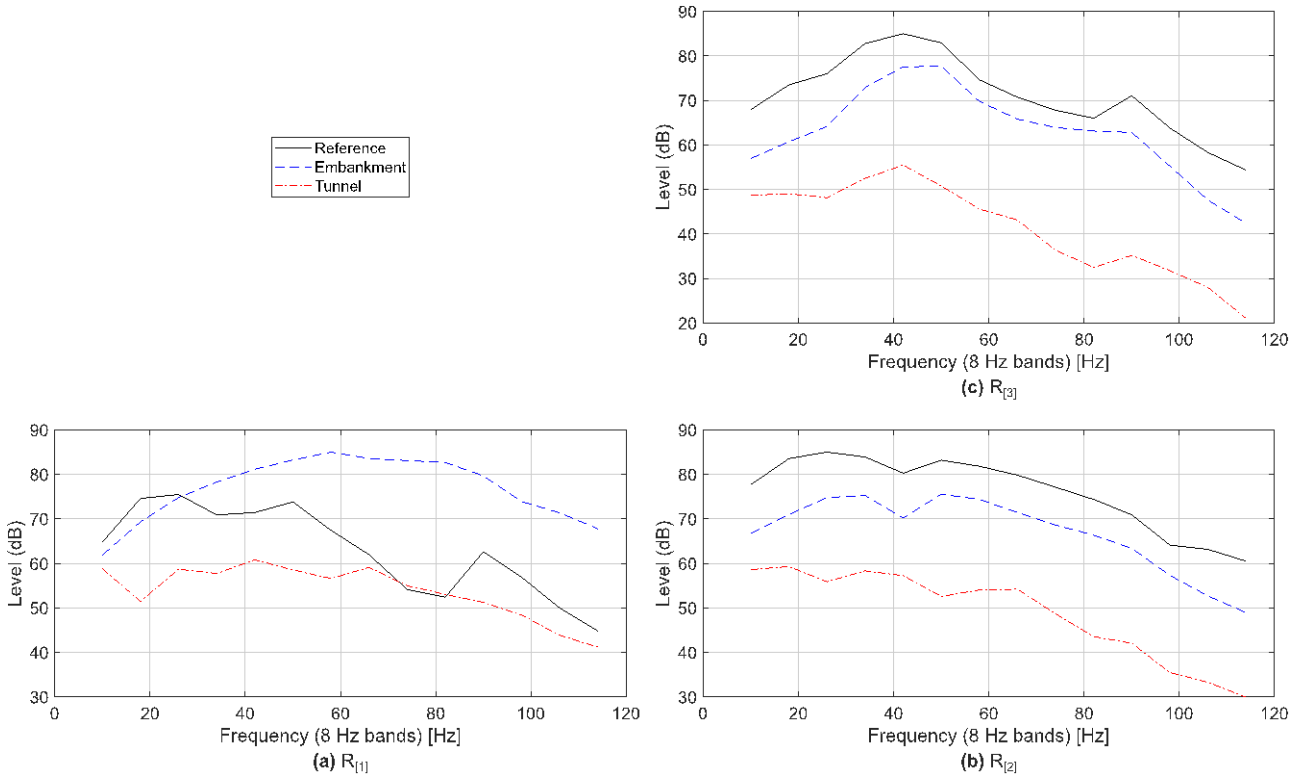
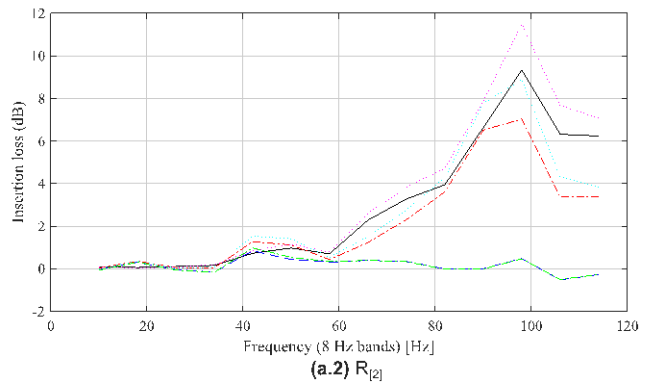
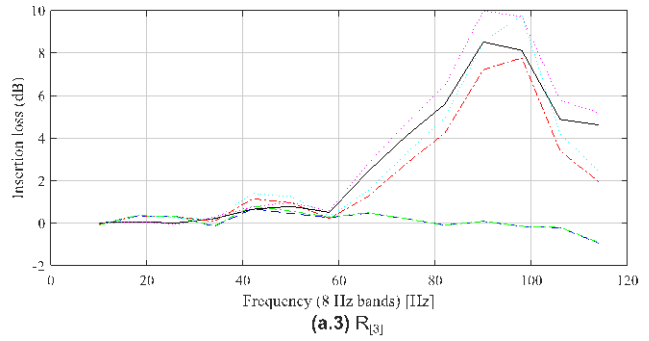
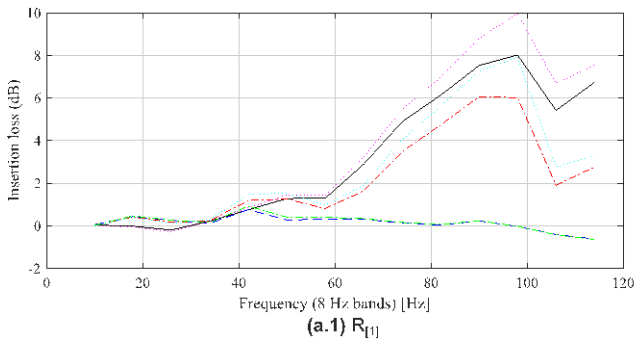
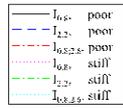


Figure 5 – Average of vertical vibration levels on different sets of receivers: (a) $R_{[1]}$, (b) $R_{[2]}$ and (c) $R_{[3]}$.

Starting by analysing the sets of phononic crystals, (see Figure 6) it is verified their low attenuation up to the central frequency of 60 Hz. The first important observation is that in the case of the embankment model – see Figure 6 (a) –, there is an attenuation peak around 90 Hz. This frequency range seems to match what is usually considered as the band gap frequency (f) in sonic crystals ($f = c/2d$) which should occur in this case around 88 Hz, if P waves are considered, propagating in the host soil with an approximate velocity of $v_p = c = 318$ m/s, and considering that the inclusions are equally spaced of $d = 1.8$ m. Performing the same calculation for S and R waves, frequencies of 44 Hz and 41 Hz are obtained, respectively. In the same figure, a less pronounced attenuation around these frequencies is also seen. Still in the case of the embankment model, it appears that the inclusion group $I_{2,2}$ has no effect. However, there are attenuation peaks, although slight, in those frequency bands previously defined as band gap. This group is at a depth of 2.2 m, very close to the wavelength of waves S ($\lambda = 2.6$ m) and R ($\lambda = 2.5$ m). On the other hand, P waves ($\lambda = 5.3$ m) perform 3.5 cycles when they reach the centre of the inclusion group and, therefore, these also propagate above or below the phononic crystal. That is, this phononic crystal, due to its location and geometry, does not interfere with the wave path. Therefore, in this model, the further up the inclusions are positioned, the more efficient the mitigation device. In the case of the tunnel model, in $R_{[1]}$ receivers – see Figure 6 (b.1) –, there is a relative optimization of groups $I_{2,2}$ and $I_{0,8,2,6}$ for the central frequencies above 70 Hz. The group $I_{0,8,2,6}$ has an attenuation loss around 90 Hz. At this frequency, Bragg interference should be felt. However, the phononic crystal is located outside the trajectory of the waves originating at the bottom of the tunnel that propagate to the receivers, therefore, they do not interfere with the path of these waves. Unlike the embankment model, in this model, the mitigation devices should be placed lower to have a better performance.

(a) Embankment



(b) Tunnel

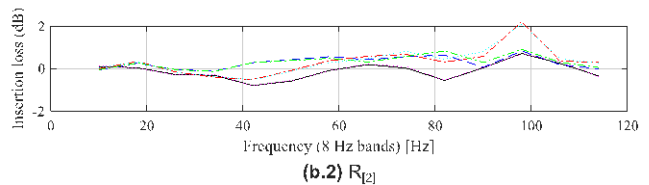
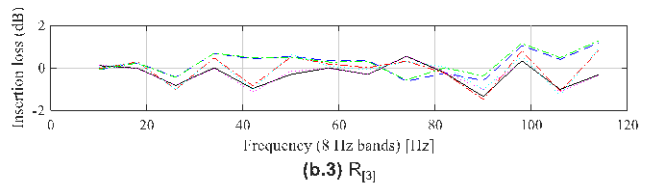
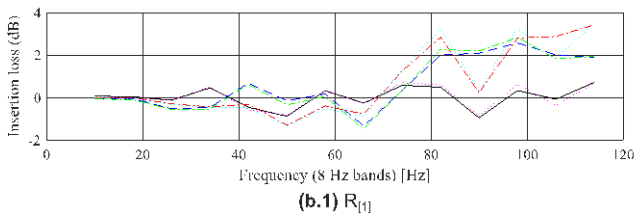
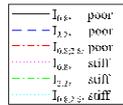
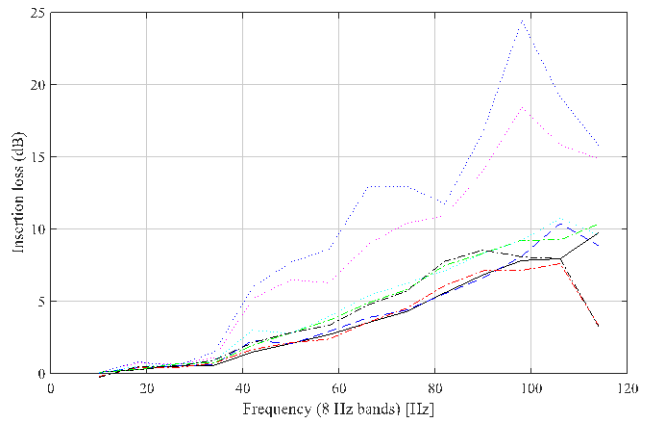
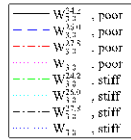


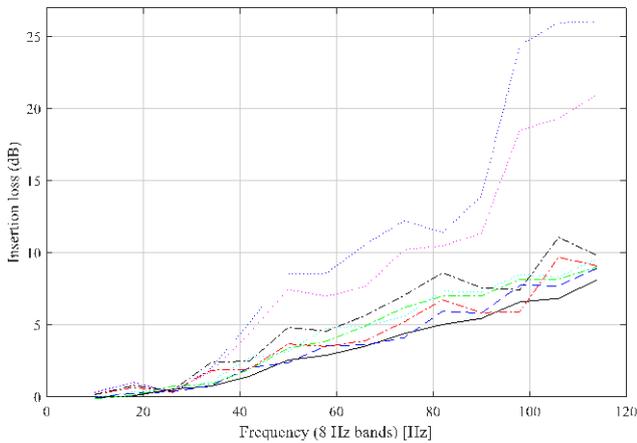
Figure 6 – Average insertion loss of inclusion groups in receivers groups (1) $R_{[1]}$, (2) $R_{[2]}$ and (3) $R_{[3]}$, whose propagation source is located in (a) embankment and (b) tunnel.

Buried walls have an increasing efficiency over frequency in the embankment model – see Figure 7 (a). As expected, the set of 3 walls, $W_{3,0}$, stands out. This is because the buried walls, which extend from the ground surface to a certain depth, are an excellent barrier to surface waves. In the tunnel model, due to its geometry, the strongest waves originating at the base of the tunnel propagate under and to the right of the mitigating devices and move upwards in the building location. This is the main reason why mitigating devices have no effect or have a negative effect on building protection – see Figure 7 (b). From Figure 7 (b.2) this conclusion can be drawn, since the single wall positioned farthest to the right, $W_{3,0}^{27,8}$, produces more attenuation than the others single walls.

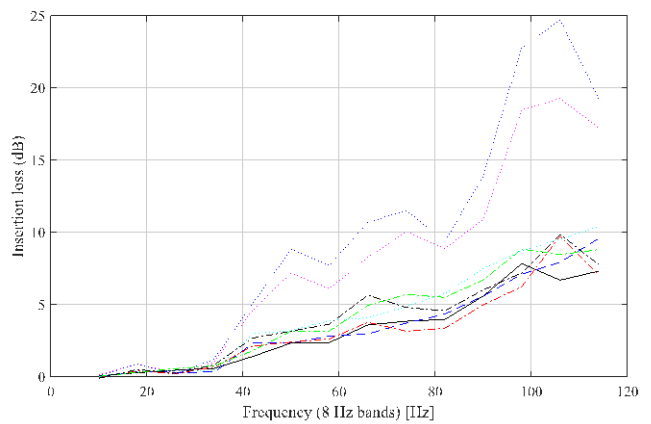
(a) Embankment



(a.3) $R_{[3]}$

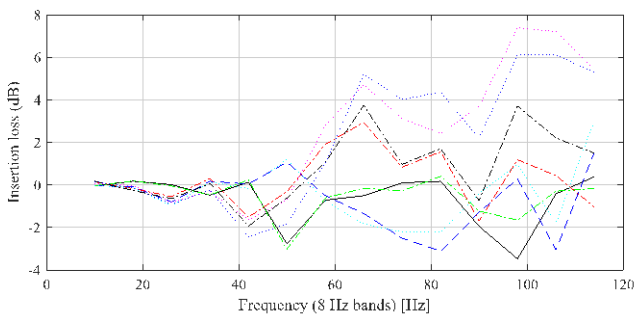
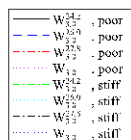


(a.1) $R_{[1]}$

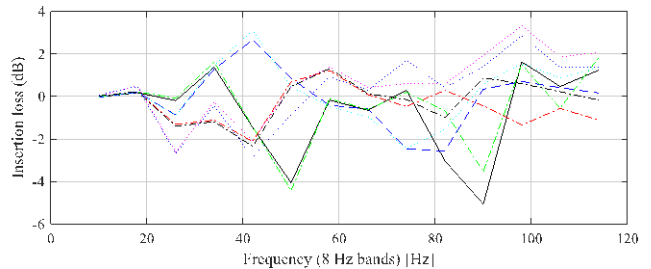


(a.2) $R_{[2]}$

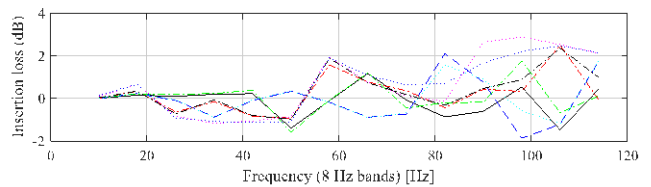
(b) Tunnel



(b.1) $R_{[1]}$



(b.3) $R_{[3]}$

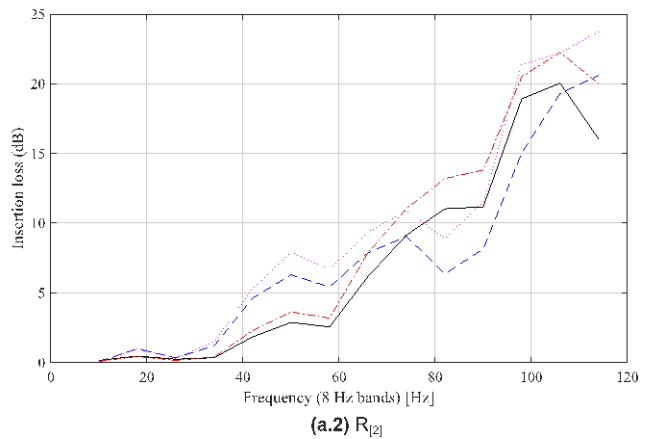
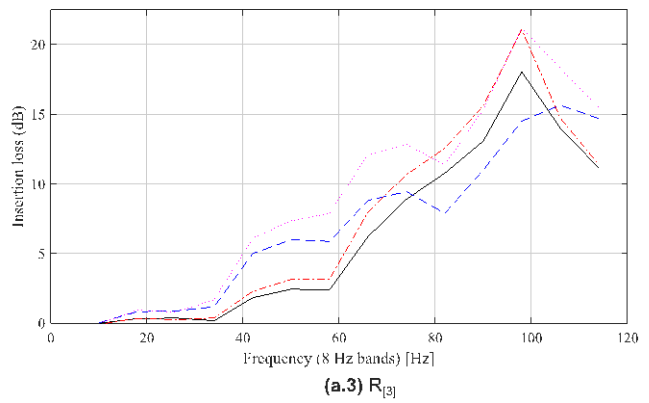
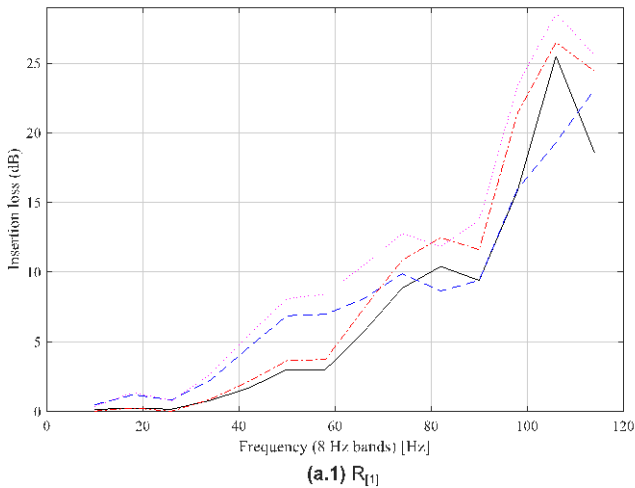
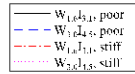


(b.2) $R_{[2]}$

Figure 7 – Average insertion loss of buried walls in receivers groups (1) $R_{[1]}$, (2) $R_{[2]}$ and (3) $R_{[3]}$, whose propagation source is located in (a) embankment and (b) tunnel.

The grouping of buried walls and inclusions (see Figure 8) achieves greater efficiency when this type of mitigating device is compared to just buried walls. Generally, in the case of embankment model – see Figure 8 (a), the stiffer mitigating devices have better performance, while in the case of the tunnel model – see Figure 8 (b), it is the depth of the mitigating devices that has better efficiency. Also, in the case of the tunnel model, there is an increase in efficiency from the central frequency of 60 Hz and, it is always positive.

(a) Embankment



(b) Tunnel

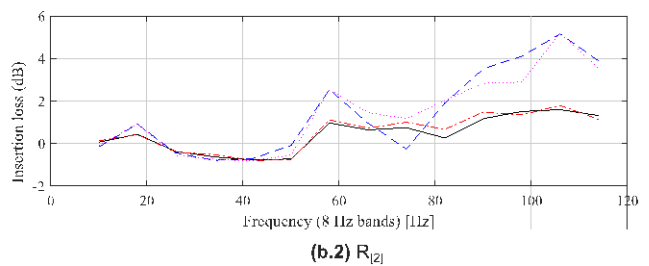
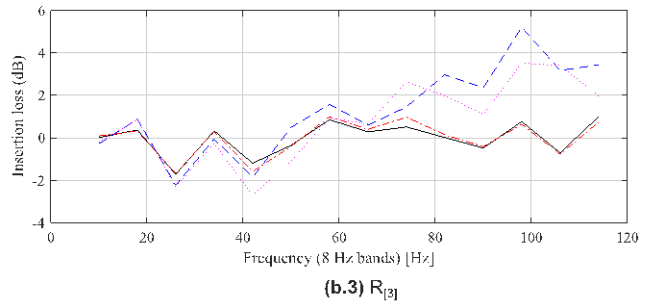
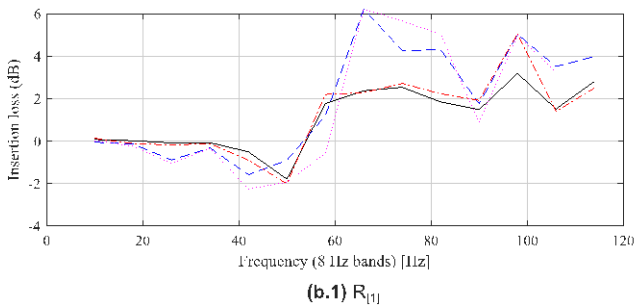
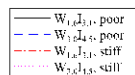
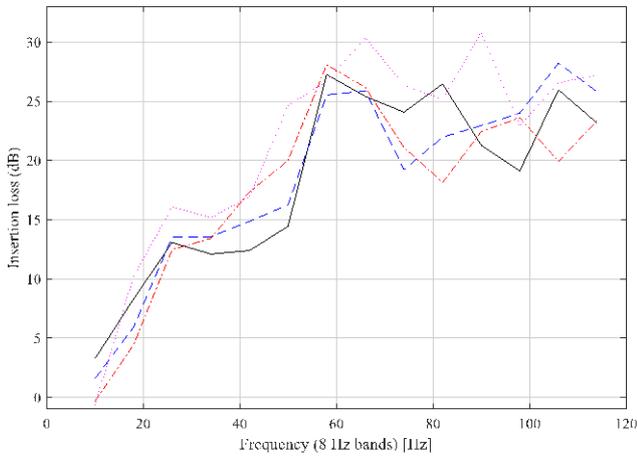


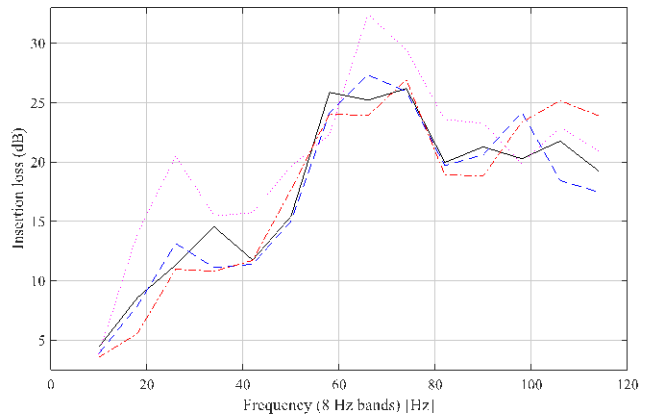
Figure 8 – Average insertion loss of buried walls and inclusions groups in receivers groups (1) $R_{[1]}$, (2) $R_{[2]}$ and (3) $R_{[3]}$, whose propagation source is located in (a) embankment and (b) tunnel.

Finally, the trenches, in the case of the embankment model – see Figure 9 (a), have a marked increase in efficiency up to the central frequency of 60 Hz and then, generally, lose some efficiency and stabilize. In building receivers – see Figure 9 (a.2) and (a.3), the loss is relatively high between the central frequencies of 75 Hz and 100 Hz in all trench models. In the tunnel model – see Figure 9 (b), similarly to the other mitigation devices, the efficiency is not relevant when compared to the embankment model.

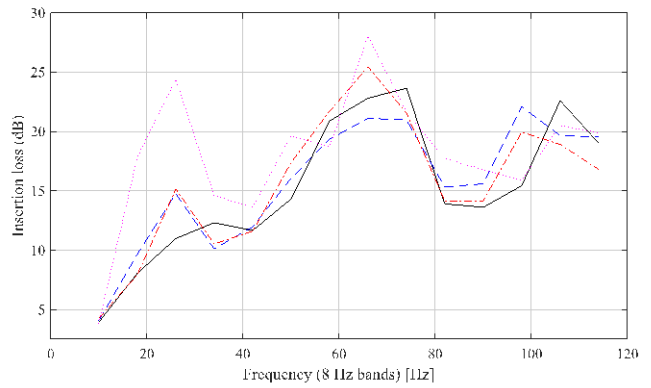
(a) Embankment



(a.1) $R_{[1]}$

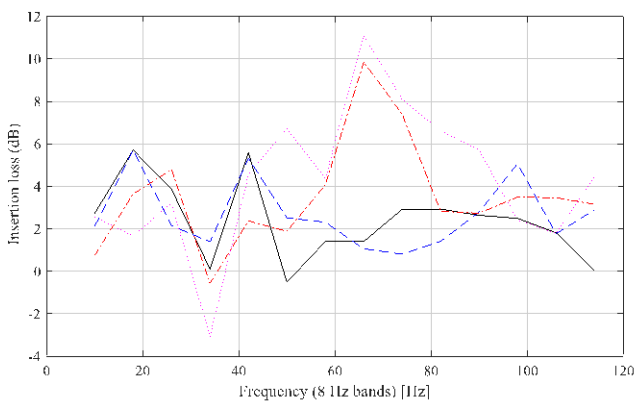


(a.3) $R_{[3]}$

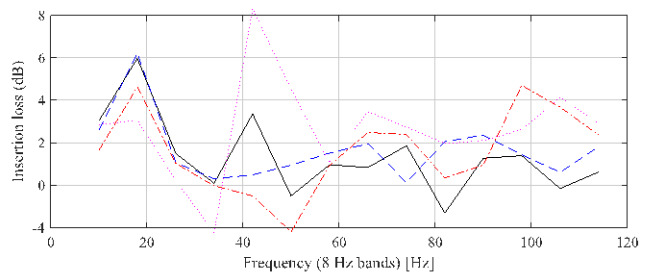


(a.2) $R_{[2]}$

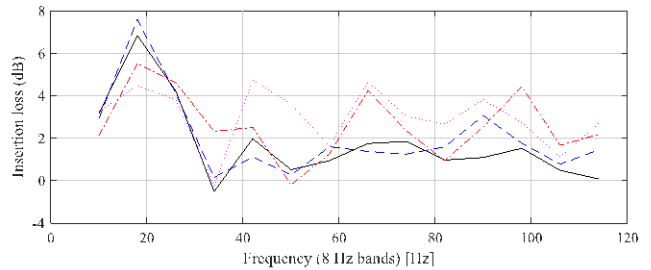
(b) Tunnel



(b.1) $R_{[1]}$



(b.3) $R_{[3]}$



(b.2) $R_{[2]}$

Figure 9 – Average insertion loss of trenches in receivers groups (1) $R_{[1]}$, (2) $R_{[2]}$ and (3) $R_{[3]}$, whose propagation source is located in (a) embankment and (b) tunnel.

5 Conclusions

This paper follows on from previous studies. The simple phononic crystals used in this study are efficient in a certain frequency range called the band gap frequency, when P waves are considered.

In the case of embankment model, mitigation devices, are very efficient as they are in the path of wave propagation. All mitigation devices show increasing efficiency with frequency except for trenches which have a drop in efficiency from the central frequency of 60 Hz.

In the tunnel model, the same mitigation devices are not as efficient as they are not in the direct path between the source and the receivers. In some cases, negative attenuation is registered as a consequence of multiple reflections of different wave types between the building and the mitigation devices.

Acknowledgements

This work was financially supported by Project POCI-01-0145-FEDER-029577 (NVTRail) funded by FEDER funds through COMPETE2020 and by national funds through FCT/MCTES (PIDDAC), and partly financed by FCT/MCTES through national funds (PIDDAC) under the R&D Unit Institute for Sustainability and Innovation in Structural Engineering (ISISE), under reference UIDB/04029/2020.

References

- [1] C. Albino, L. Godinho, P. Amado-Mendes, P. Alves-Costa, D. Dias-da-Costa, D. Soares Jr., 3D FEM analysis of the effect of buried phononic crystal barriers on vibration mitigation, *Eng. Struct.* 196 (2019) 109340. doi:<https://doi.org/10.1016/j.engstruct.2019.109340>.
- [2] C. Albino, Numerical Simulation of Elastic Wave Propagation in Discontinuous Media: applications in ultrasonic and vibration control, University of Coimbra, 2021. <http://hdl.handle.net/10316/95285>.
- [3] P. Amado-Mendes, L.M.C. Godinho, Reduction of vibrations transmitted through the soil by multiple buried inclusions – numerical analysis, in: Z. Dimitrovová, et al. (Eds.), 11th Int. Conf. Vib. Probl., Lisboa, 2013.
- [4] C. Albino, L. Godinho, D. Dias-da-Costa, P. Amado-Mendes, The MFS as a tool for the numerical analysis of vibration protection devices, in: 22nd Int. Congr. Acoust. (ICA 2016), Buenos Aires, 2016.
- [5] L. Godinho, P. Amado-Mendes, P. Alves-Costa, C. Albino, MFS analysis of the vibration filtering effect of periodic structures in elastic media, *Int. J. Comput. Methods Exp. Meas.* 6 (2018) 1108–1119. doi:10.2495/CMEM-V6-N6-1108-1119.
- [6] A. Castanheira-Pinto, P. Alves-Costa, L.M.C. Godinho, P. Amado-Mendes, Mitigation of vibrations induced by railway traffic through soil buried inclusions: a numerical study, in: A. Calvo-Manzano, A. Pérez-López (Eds.), 48° Congr. Español Acústica (TECNIACÚSTICA 2017), A Coruña, 2017: pp. 1078–1086.
- [7] D. Soares Jr., A novel family of explicit time marching techniques for structural dynamics and wave propagation models, *Comput. Methods Appl. Mech. Eng.* 311 (2016) 838–855. doi:<http://dx.doi.org/10.1016/j.cma.2016.09.021>.